Can. J. Remote Sensing, Vol. 28, No. 3, pp. 484–489, 2002

Investigation of C-band altimeter cross section dependence on wind speed and sea state

J. Gourrion, D. Vandemark, S. Bailey, and B. Chapron

Abstract. Wind and wave impacts on C-band altimeter backscatter data are presented using data collected from the TOPEX/POSEIDON platform. The compilation of a large global data set of TOPEX observations collocated with NASA scatterometer (NSCAT) wind speed estimates is used to propose an algorithm for wind speed retrieval using both cross section and significant wave height observations. Evidence of sea state impact on radar backscatter is further analyzed through comparison with National Oceanographic Data Center (NODC) buoy spectral wave measurements. For wind speeds above 6 $m \cdot s^{-1}$ and global mean sea state conditions, altimeter and buoy-derived slope variance estimates exhibit high correlation in their wind speed and sea state dependencies. Results suggest that the C-band instrument may be used to derive new data on the degree of development of the sea state.

Résumé. On montre les impacts du vent et des vague sur les données de rétrodiffusion altimétrique en bande C à l'aide des données acquises par la plate-forme TOPEX/POSEIDON. Basé sur la compilation d'un vaste ensemble de données à l'échelle du globe dérivées des observations TOPEX co-localisées avec les estimations de vitesse de vent NSCAT, on propose un algorithme d'extraction de la vitesse du vent utilisant des données sur la section radar efficace et la hauteur significative des vagues. L'évidence de l'impact de l'état de surface de la mer sur la rétrodiffusion radar est analysée de façon plus approfondie à l'aide d'une comparaison avec des mesures de spectres de vagues obtenues à partir des bouées NODC. Pour des vitesses de vent supérieures à 6 $m \cdot s^{-1}$ et dans des conditions globales moyennes d'état de surface de la mer, les estimations de la pente quadratique moyenne dérivées de altimètre et des bouées montrent une forte corrélation dans leur dépendance par rapport à la vitesse du vent et l'état de surface de la mer. Les résultats suggèrent que l'instrument en bande C est utile pour dériver des nouvelles données sur l'état de développement de l'état de surface de la mer.
[Traduit par la Rédaction]

Introduction

The TOPEX C- and Ku-band altimeters have been observing the ocean surface topography for nearly 10 years. Both instruments provide simultaneous significant wave height (H_S) and radar cross section (σ^o) estimates. These are presently used to empirically adjust the altimeter range measurement, but also to provide independent wind speed inversion for calibration–validation purposes. Numerous studies in the past 20 years have addressed the design of Ku-band wind speed model functions (Brown et al., 1981; Witter and Chelton, 1991; Glazman and Greysukh, 1993; Freilich and Challenor, 1994; Gourrion et al., 2002a).

The C-band instrument, primarily designed for Ku-band corrections of ionospheric path delay, has not received the same attention as its Ku-band companion. Several studies have suggested that combined C- and Ku-band cross section measurements might lead to improved accuracy in wind speed inversion (Bliven et al., 1996; Chapron et al., 1995; Elfouhaily et al., 1997). These studies, among others, conclude that the main limitation to the accuracy of the retrieved wind speed is the lack of accurate simultaneous information on sea state. To further exploit the altimeter observations, this paper focuses on the description of C-band cross section under various wind speed and sea state conditions.

An outline of the paper is given as follows. The first section of the paper briefly presents a two-parameter (σ^o, H_S) wind speed algorithm for C-band instruments. This model function was designed using the same neural network approach as that of the JASON Ku-band operational algorithm (Gourrion et al., 2002a). It is more thoroughly described in a report by Gourrion et al. (2000). The paper demonstrates that C-band backscatter is less (more) correlated with wind speed (sea state) than is observed at Ku band. Following a climatological description of long-wave acceleration estimates as a function of wind speed and H_S is presented using National Oceanographic Data Center (NODC) buoy measurements. The large TOPEX/NSCAT data set described in the algorithm development is used to compare a climatological C-band derived mean square slope (mss) parameter with the preceding buoy-derived acceleration variance climatology. The domain of validity of the preceding identification is pointed out, followed by a summary of the conclusions.

Received 17 January 2002. Accepted 10 March 2002.

J. Gourrion[1] and B. Chapron. Institut Français de Recherche pour l'Exploitation de la Mer (IFREMER), Département d'Océanographie Spatiale, BP 70, 29280 Plouzané, France.

D. Vandemark and S. Bailey. National Aeronautics and Space Administration (NASA), Goddard Space Flight Center, Wallops Island, VA 23337, U.S.A.

[1]Corresponding author (e-mail: gourrion@wanadoo.fr or gourrion@ifremer.fr).

Observations and wind speed model

Taking advantage of high-resolution (25 × 25 km) NASA scatterometer (NSCAT) wind products (similar time and space resolutions, global representability, and large amount of data in comparison to collocation with buoy observations or meteorological model prediction) (Dunbar, 1997), we created a global collocated data set from TOPEX altimeter data ("MGDRB", Benada, 1997; "HR-MGDR", Dunbar, 1997). TOPEX data are provided as 1 s averages, corresponding to about a 2 × 6 km ground track. We then averaged these data along track to extend the spatial footprint out to 2 × 25 km such that the spatial match is closer to the NSCAT footprint. The collocation was run over the whole advanced Earth observation satellite (ADEOS; NSCAT platform) life, from September 1996 to June 1997. The maximum prescribed distance between the two observations is 15 km, and maximum time lag is 60 min; 245 000 collocated points were obtained. Sea state impacts on the scatterometer wind speed are assumed negligible based on numerous studies (see Nghiem et al., 1997). Recent global study (Queffeulou et al., 1999) has shown that a measurable sea state effect can be seen in lower angle NSCAT data, but also that the larger angle scatterometer data do not exhibit significant correlation. Consequently, only those NSCAT winds where the observation angle exceeded 40° were accepted, giving a final selection of 96 500 samples. The expectation is that this will reduce possible sea state impacts on scatterometer winds to levels acceptable for altimeter model study. Validations using buoy and wind forecast data shown in Gourrion et al. (2000) indicate that this is the case.

Figure 1 shows the overall H_S influence for given U_{NSCAT} and σ_C^0 bins. For a wind speed of 6 m·s^{-1}, we observed a σ_C^0 variation of 2 dB between low and high sea states. This is equivalent to a wind speed variation of about 10 m·s^{-1} when using a backscatter-only C-band altimeter retrieval such as the algorithm presented in the next paragraph (and shown as a solid line in **Figure 1**).

The C-band cross section appears strongly dependent on sea state. To derive a wind speed algorithm, the simultaneous H_S information should be accounted for. Neural-network methods were used to provide an empirical bivariate model function. Method, validation, and algorithm (Gourrion et al., 2000) are available at <http://www.ifremer.fr/droos/Perso/gourrion/rapport/rapport.html> or <http://topex.wff.nasa.gov/docs/docs.html>. **Figure 2** shows the wind error dependence on H_S for two different algorithms. The one-parameter wind speed algorithm can be considered as the C-band equivalent to the Ku-band algorithm from Witter and Chelton (1991). By including H_S information, the two-parameter algorithm helps to

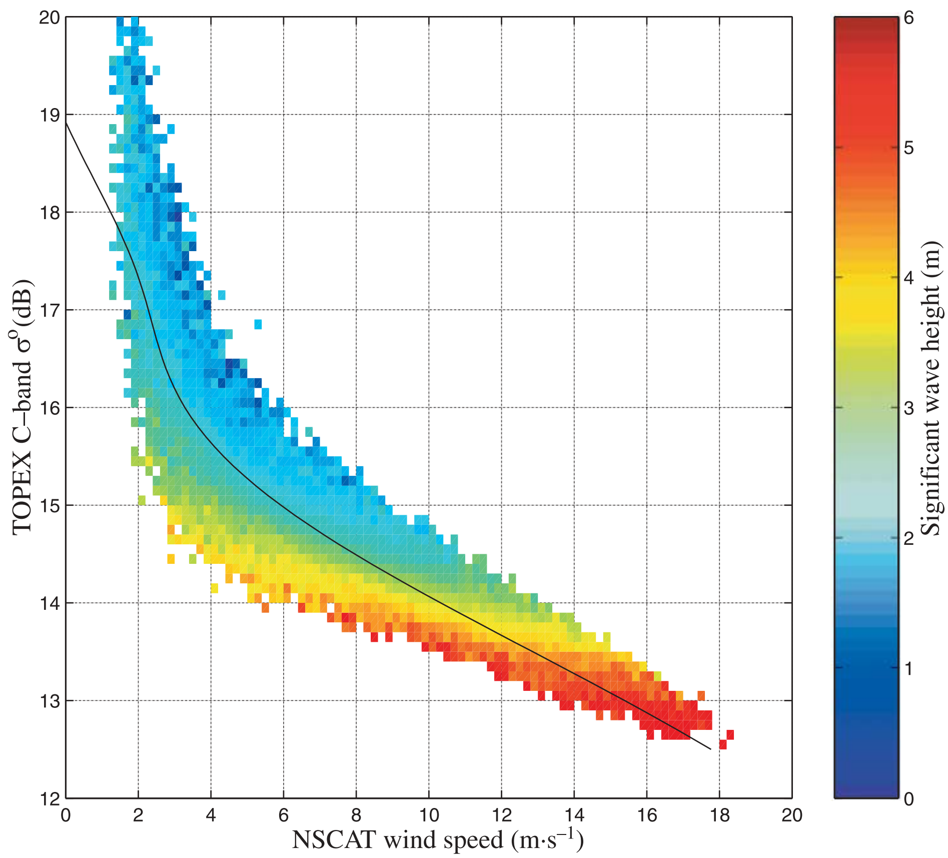

Figure 1. Gridding of the TOPEX σ_C^0 and NSCAT wind speed. The color represents the corresponding average H_S estimate. The population consists of 91 834 data points, with a minimum of 5 per bin.

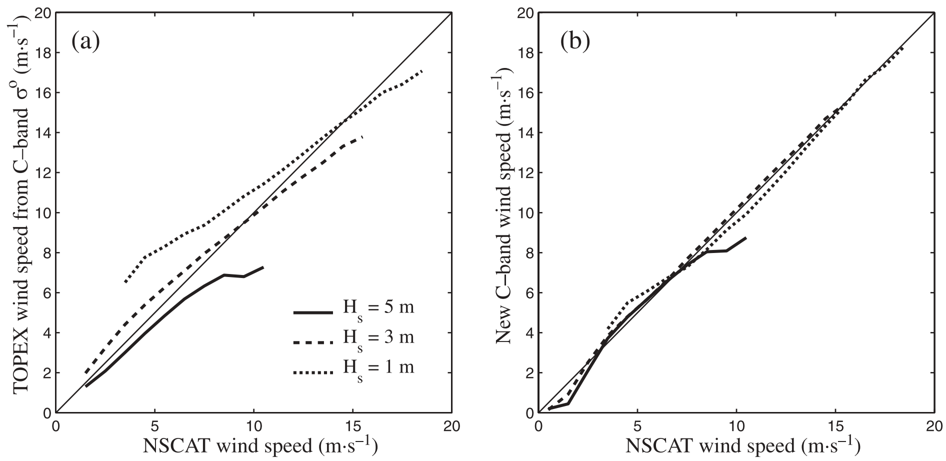

Figure 2. Averaged altimeter wind speed estimate as a function of NSCAT wind speed for significant wave heights H_S = 1, 3, and 5 m: (a) standard one-parameter C-band altimeter algorithm; (b) new two-parameter C-band altimeter algorithm.

significantly reduce the sea state induced wind error. For this NSCAT/TOPEX data set, the root-mean-squared (rms) wind error is reduced by 10%, from 1.25 to 1.12 $m \cdot s^{-1}$. The absolute wind error levels are slightly higher than those obtained for the analogous Ku-band inversion model. This is because the C-band σ_0 is a priori less correlated with the local wind (e.g., Chapron et al., 1995). The relative improvement obtained by including H_S is slightly greater at Ku band (15%) than at C band (10%). This may seem physically counterintuitive, but results from the fact that the wind algorithms discussed here are inverse and not forward models. In this case, it is the level of independence between input variables that dictates wind error reduction levels. Since Ku-band σ_0 is relatively less dependent on H_S, this inversion will make better use of H_S.

As the C-band cross section data appear less correlated with wind speed and more correlated with sea state (through H_S) than at Ku band, the correlation between C-band cross section and H_S is now examined through comparison with in situ buoy spectral observations by using a climatological approach. One primary concern in this approach is deriving a buoy data climatology with mean swell and slope characteristics that is reasonably consistent with that from the global altimeter – scatterometer sampling domain for given wind speed and H_S bins. This is discussed in the following section.

Climatology of buoy-derived acceleration variance

We used wind speed and wave measurements of moored buoys from the National Oceanographic Data Center (NODC) of the National Oceanic and Atmospheric Administration (NOAA). The buoys presently used are from six different regions in the United States: Western Atlantic (41001, 41002, 44004, 44008, 44011), Great Lakes (45001–45008), Gulf of Mexico (42019, 42020, 42036, 42039, 42040), Hawaii (51001–51004), Eastern Pacific (46002, 46005, 46006, 46059), and Alaska (46001, 46003, 46066). Observation areas span from low to high latitudes and from closed seas and lakes to open basins.

These buoys provide hourly 10 min averaged wind speeds (measured at 5 m height) and frequency elevation spectra up to f_{cut} = 0.4 Hz, corresponding roughly to waves longer than 10 m (some spectra provided up to 0.5 Hz were truncated to 0.4 Hz). Long-wave acceleration variance (denoted MSA in the following for mean square acceleration) are estimated from the individual hourly elevation spectra $S(f)$ as follows:

$$\mathrm{MSA} = \int_0^{f_{\mathrm{cut}}} f^4 S(f) \mathrm{d}f \tag{1}$$

A climatological wave height and wind speed covariance with the vertical acceleration variance is then regionally estimated by averaging the individual values for given wind speed and significant wave height bins. To ensure statistical significance, a minimum of 10 events is required to compute any average.

The results are presented in **Figure 3**. Between 80 000 and 235 000 individual spectra were used in each zone. At first order, one sees the expected increase of MSA with increasing wind speed for all cases. Substantial MSA variation with H_S is also apparent in all data sets. Particular wind–wave climatological characteristics are also observed between data collection regions. For the Hawaiian data, MSA depends less on H_S, suggesting that the longer swell dominates H_S but only weakly modifies MSA. The Hawaiian MSA climatology is likely typical of intertropical regions where the swell signature is generated by distant high-latitude storms that propagate energy towards the equator. The average swell characteristics associated with a given zone are best obtained by examining the lowest wind speed range where the wind-wave field contribution is lowest. Hawaiian data display characteristics of long gentle swell while the other data sets here contain more

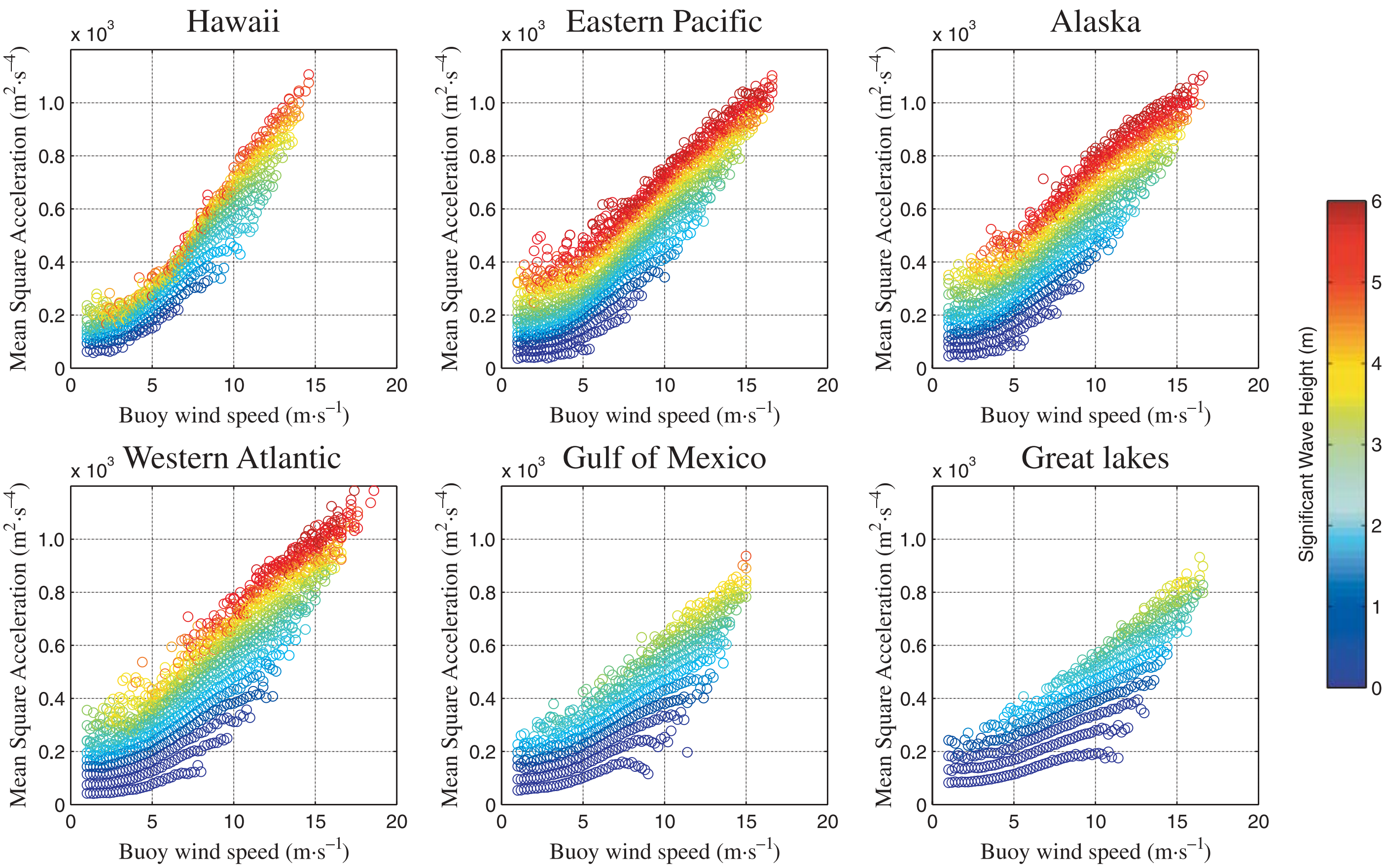

Figure 3. Climatological average of the NDBC-derived long-wave acceleration variance as a function of buoy wind speed and H_S for six different NODC regions: Hawaii, Alaska, Eastern Pacific, Western Atlantic, Gulf of Mexico, and Great Lakes.

frequent occurrences of steeper background waves corresponding to younger swell, i.e., waves generated closer to the area of interest or at a shorter time before the observation. The Gulf of Mexico and Great Lakes data display stronger variations of MSA with H_S at the lowest sea states. They give greater weight to early developing wind sea conditions and provide little low wind – high sea state observations. These two data sets similarly describe closed-basin conditions. The Eastern Pacific, Alaska, and Western Atlantic data sets exhibit similar MSA characteristics for a wide range of wind speeds and sea states. They only differ for the infrequent extreme sea conditions: the Eastern Pacific provides more low wind – high sea state cases, and the Western Atlantic contains sensibly more high wind – low sea state cases (consistent with the fact that the dominant westerly winds blow from the shore in the Western Atlantic).

Although the Hawaiian climatology overweights swell-contaminated sea states and the climatology of both the Gulf of Mexico and the Great Lakes favor young, developing wind sea conditions, the high consistency between the MSA characteristics in the Eastern Pacific, Alaska, and Western Atlantic data sets suggests that they provide a reasonably representative picture of the overall mean conditions. Consequently, it is assumed that a NODC-inferred global mean MSA can be obtained from any of these three data sets. The Alaskan data set is used in the following comparison.

Comparison of climatological altimeter and buoy data

To evaluate the impact of longer waves ($\lambda > 10$ m) on the C-band cross section, we need some climatology for both σ^o_C and buoy slope variance mss_L. Using the linear gravity wave dispersion relation, the buoy-derived slope variance (mss_L) climatology is deduced from the preceding buoy acceleration variance MSA:

$$\mathrm{mss}_L = \frac{(2\pi)^4}{g^2}\mathrm{MSA} \tag{2}$$

where g is the acceleration due to the Earth's gravity.

The altimeter cross section climatology is obtained from the extensive NSCAT/TOPEX data set briefly presented earlier in the paper. Using a simple geometrical model (e.g., Brown, 1978), the measured C-band cross section relates to an altimeter-derived sea slope variance (mss_C) parameter as follows:

$$\mathrm{mss_C} = \frac{K}{\sigma^o_C} \tag{3}$$

where K is a proportionality constant; here it includes the Fresnel reflection coefficient, slope statistical description, and possible radar calibration offset. In the absence of the last two pieces of information, K is set to 0.64, the nominal Fresnel coefficient value.

Figure 4 shows comparisons between the NDBC-derived simple prediction and the global altimeter slope variance for different H_S values. To aid visual comparison, the buoy-derived parameter has been shifted upward by 0.015 in **Figure 4b**. As suggested in the previous section, the Eastern Pacific, Alaska, and Western Atlantic data sets are very consistent in their open ocean buoy acceleration variance estimates. Considering that the global altimeter set is weighted towards offshore areas, including increased importance of high-latitude zones due to the present collocation process, these three data sets, among the six listed, provide the best possibility of altimeter–buoy comparisons. The Alaskan data set is used for this plot, but the two other sets provide very similar results.

Discussion

Figure 4 clearly depicts a strong correlation between C-band altimeter- and buoy-derived slope variance for the wide range of sea state conditions. For wind speeds lower than 6 m·s^{-1}, the non-zero but near-constant buoy mss reflects the climatological background swell level (see the climatology section) and the fact that any wind-related surface roughness is associated with short scales not sampled by the buoy system. For wind speeds above 6 m·s^{-1}, observations suggest that, for moderate to high wind speed, the global mean C-band cross section characteristics should be predictable from buoy spectral tail measurements, that is from gravity wave slope characteristics for waves larger than about 10 m. The only information lacking here is an offset parameter; as demonstrated in **Figure 4**, however, this offset parameter can be set to a constant value of the order 1.5e^{-2}. Both measurements, although of a much different nature (in situ versus remote), are similarly impacted by wind speed and sea state, except in the case of low wind speed conditions. This result shows that, although not immediate, the C-band mss comparison to MSA is sensible. It also demonstrates that the mean buoy regional H_S–MSA–U_5 and altimeter global H_S–MSS–U_{10} domains are quite similar, where U_{10} (U_5) is the wind speed at a height of 10 m (5 m). The result further suggests that a hypothetical TOPEX/NSCAT collocation data set exclusively over the Hawaiian case or the closed-basin NODC cases should end up looking like the NODC H_S–MSA–U_{10} domain.

The climatological approach does not allow the interpretation of this result in terms of a point-by-point analysis. In deriving the five relations of **Figure 4**, data were binned in the space (U_{10}, H_S); a minimum number of points (25) was used to ensure statistical significance. Consequently, the events with low occurrence (such as young sea states under moderate to high wind speeds) are weighted weakly in this analysis. Such events are analyzed by Gourrion et al. (2002b) using FETCH (Flux, Etat de la mer et Télédétection en Conditions de fetcH variable) campaign data. Therefore, it should be kept in mind that the observations of the preceding section mainly concern fully developed wind seas or mixed sea and swell conditions under moderate to high wind speeds.

Conclusions

A significant impact of significant wave height on the C-band altimeter cross section measurement has been demonstrated using a global data set. An empirical two-parameter algorithm for C-band altimeter wind speed retrieval was developed to lower this systematic H_S effect. We further

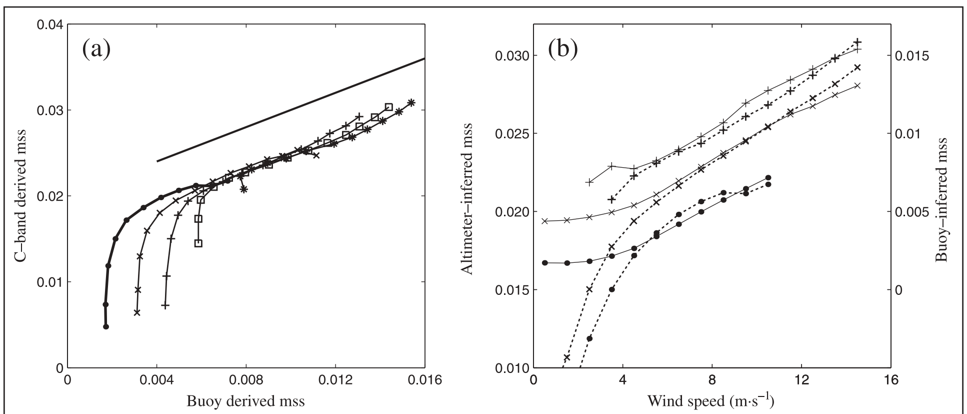

Figure 4. Comparison of global C-band inferred and NODC-derived slope variance parameters for different H_S values. (a) Five H_S values are selected: 1 m (●), 2 m (×), 3 m (+), 4 m (□), and 5 m (*). A straight line with slope 1 is shown for comparison. (b) The buoy-derived (solid lines, right axis) and altimeter-derived (broken lines, left axis) slope variance parameters are plotted separately as a function of wind speed for three H_S values: 1 m (●), 3 m (×), and 5 m (+). Note that the right axis is shifted up by 0.015.

demonstrate that the in situ measure of longer (>10 m) gravity wave acceleration can be used to explain most of the wind speed and H_S dependencies of C-band altimeter returns above 6 m·s^{-1}. This statement applies in a global mean sense. The results suggest that C-band measurements contain valuable information that could potentially be used to better characterize the degree of development of the sea state and extend buoy-derived findings to the global scale.

This may be of great interest in future exploitation of altimeter data (particularly the Ku-band wind speed inversion) and Global Navigation Satellite System L-band bistatic quasi-specular sea surface reflected signals. In the immediate future, the S-band (9 cm) ENVISAT altimeter should help to confirm these observations.

References

Benada, R. 1997. *Merged gdr (topex/poseidon) generation b: user's handbook*, version 2.0. JPL D-11007. Physical Oceanography Distributed Active Archive Center (PO-DAAC), Jet Propulsion Laboratory, California Institute of Technology, Pasadena, Calif.

Bliven, L.F., Sobieski, P., Guissard, A., and Branger, H. 1996. Friction velocity estimation using dual-frequency altimeter. In *The air–sea interface*. Edited by M.A. Donelan, W.H. Hui, and W.J. Plant. The University of Toronto Press, Toronto, Ont. pp. 686–691.

Brown, G.S. 1978. Backscattering from a gaussian distributed, perfectly conducting, rough surface. *IEEE Transactions on Antennas and Propagation*, Vol. AP-26, pp. 472–482.

Brown, G.S., Stanley, H.R., and Roy, N.A. 1981. The wind speed measurement capability of spaceborne radar altimeters. *IEEE Journal of Oceanic Engineering*, Vol. OE-6, No. 2, pp. 59–63.

Chapron, B., Katsaros, K., Elfouhaily, T., and Vandemark, D. 1995. A note on relationships between sea surface roughness and altimeter backscatter. In *Air–water gas transfer: selected papers from the third international symposium on air-water gas transfer.* Edited by B. Jähne and E.C. Monahan. AEON Verlag & Studio, Hanau, Germany. pp. 869–878.

Dunbar, R.S. 1997. *Nasa scatterometer, high-resolution merged geophysical data products*. JPL D-14560, Physical Oceanography Distributed Active Archive Center (PO-DAAC), Jet Propulsion Laboratory, California Institute of Technology, Pasadena, Calif.

Elfouhaily, T., Chapron, B., Vandemark, D., and Gourrion, J. 1997. Estimation of wind stress using dual-frequency TOPEX data. *Journal of Geophysical Research*, Vol. 103, No. C11, pp. 25 101 – 25 108.

Freilich, M.H., and Challenor, P.G. 1994. A new approach for determining fully empirical altimeter wind speed model functions. *Journal of Geophysical Research*, Vol. 99, No. C12, pp. 25 051 – 25 062.

Glazman, R.E., and Greysukh, A. 1993. Satellite altimeter measurements of surface wind. *Journal of Geophysical Research*, Vol. 98, pp. 2475–2483.

Gourrion, J., Vandemark, D., Bailey, S., and Chapron, B. 2000. Satellite altimeter models for surface wind speed developed using ocean satellite crossovers. Technical Report IFREMER-DROOS-2000-02, Institut Français de Recherche pour l'Exploitation de la Mer, Nantes, France.

Gourrion, J., Vandemark, D., Bailey, S., and Chapron, B. 2002a. A two parameter wind speed algorithm for ku-band altimeters. *Journal of Atmospheric and Oceanic Technology.* In press.

Gourrion, J., Vandemark, D., and Chapron, B. 2002b. Altimeter cross section and significant wave height data under growing sea conditions. *Journal of Geophysical Research.* In preparation.

Nghiem, S.V., Li, F.K., and Neumann, G. 1997. The dependence of ocean backscatter at Ku-band on oceanic and atmospheric parameters. *IEEE Transactions on Geoscience and Remote Sensing*, Vol. 35, No. 3, pp. 581–600.

Queffeulou, P., Chapron, B., and Bentamy, A. 1999. Comparing ku band NSCAT scatterometer and ERS-2 altimeter winds. *IEEE Transactions on Geoscience and Remote Sensing*, Vol. 37, pp. 1662–1670.

Witter, D.L., and Chelton, D.B. 1991. A geosat altimeter wind speed algorithm and a method for altimeter wind speed algorithm development. *Journal of Geophysical Research*, Vol. 96, No. C5, pp. 8853–8860.